

On the Numerical Solution and Limitations of Energy Equation for Vertical Bridgman System with Varying Temperature Gradient at the Boundary

Ergün TAŞARKUYU

*Department of Physics, Faculty of Art and Sciences, Middle East Technical University,
06531, Ankara-TURKEY*

On leave from Department of Physics, Muğla University, Muğla-TURKEY

Evren AKAR and Bülent Gültekin AKINOĞLU*

*Department of Physics, Faculty of Art and Sciences, Middle East Technical University,
06531, Ankara-TURKEY*

e-mail: bulent@newton.physics.metu.edu.tr

Received 25.05.2001

Abstract

In vertical Bridgman crystal growth systems solid-liquid interface shape is one of the most important factors affecting the product quality. Most of the theoretical studies to determine the interface shape consider the numerical solution to the heat-conduction and the energy equation. The purpose of this work is to present and discuss a numerical solution to the energy equation (also called the convection-diffusion equation) for a vertical Bridgman system with varying temperature gradient at the boundary. Different system parameters are examined and the importance of the pulling rate for different materials in the utilization of the energy equation is emphasized. The limitations and the accuracy of the energy equation in describing the interface shape are presented and discussed. A finite difference scheme is utilized for the numerical solution using different approaches to the problem and the results are obtained for different temperature profiles and crucible radii. It is observed that the slope of the axial temperature profile within the material is mainly affected by the crucible translation rate.

1. Introduction

The position and the shape of the solid-liquid (SL) interface are of primary importance as these are the main factors that determine the product quality in crystal growth processes from melt by directional solidification techniques. The shape of SL interface is often used as an indicator of the crystallographic imperfections such as the density of dislocations. Therefore, detailed numerical calculations may be extremely helpful to determine the optimum growth conditions by investigating the effects of design and operation parameters.

Numerical approaches to the solidification problem in vertical and/or horizontal Bridgman systems have appeared in the literature since the 1970s. These approaches mostly use finite-difference, finite-element, finite-volume and boundary element methods [1-13]. Some researchers use the well-known energy equation (also known as a convection- diffusion equation and its form used for specific applications in the process of crystal growth from melt, like the present work, is given in Equation (3) of the next section) as the governing equation by which some basic conclusions about the SL interface shape and position can be drawn (see, for

*Corresponding author.

example, [2], [4], [5]). In the present study a two-dimensional energy equation is solved by finite-difference method for the three zone vertical Bridgman system using varying temperature gradient at the boundary. Different approaches to the problem are carried out and the limitations of the energy equation in obtaining better estimates of the SL interface shape and position are discussed.

Chang and Wilcox [14] solved the energy equation analytically and obtained that, as the effectiveness of heat transfer between ampoule and the surroundings diminishes and as the thermal conductivity of the material increases, the SL interface position becomes more sensitive to the physical parameters and the geometry of the system. They used constant upper and lower zone temperatures to represent the upper heater and lower cooler regions of the vertical Bridgman furnace. Later, Fu and Wilcox used a numerical method to solve the energy equation for a system with insulation between the heater and cooler [2]. They concluded that the addition of an insulated region drastically decreases the sensitivity of the SL interface shape to the system parameters.

Chin and Carlson [3] solved the two-dimensional quasi-steady state heat conduction equation using finite element method by Gauss-Sidel iteration scheme for vertical Bridgman crystal growth system. Their conclusion was that the interfacial curvature was strongly influenced by material's solid-liquid thermal conductivity ratio, dimensionless interface temperature, Biot number and, to a much lesser degree, by insulation zone thickness and ampoule position. They consequently stated that the material properties must be accurately known if any predictions of the interface convexity were to yield meaningful results. They also obtained that the curvature can be made independent of furnace Biot number and ampoule position by proper choice of the dimensionless interface temperature.

Huang et al. [4] used the finite element method to solve the energy equation for a Bridgman system having temperature profiles with constant temperature gradients for the hot, transition and cold regions. They obtained that the convexity approximately varied by the log of the liquid to solid thermal conductivity ratio. They concluded that when the furnace temperature profile was considered to have a steep temperature gradient between hot and cold regions of relatively flat temperature gradient, the SL interface shape depended on the proximity to these hot and/or cold regions. Moving the interface away from the low temperature zone would decrease the tendency towards formation of a concave interface.

Young et al. [5] used the boundary element method to solve the energy equation for a horizontal Bridgman system. Their results indicated that relatively higher values of the furnace translation rate affected the shape of the SL interface (as expected), and up to the rate 5 mm/hr the shape of the SL interface was almost flat.

More recently, with the developments in computer technology, researchers started to include detailed formulations and increased number of parameters in their models. Lan and Ting [6] used the equations of motion and energy, and their associated boundary conditions formulated in terms of stream function and vorticity to simulate the growth of sodium nitrate chosen as a model material. Their furnace was a transparent multi-zone furnace with an adiabatic region between hot and cold zone controlling the temperature gradient at the SL interface. Their results about the concavity of the interface shape were in good agreement with the experimental results for three different temperature profiles at a pulling rate of 2.6 cm/hr. Interface became flatter as the imposed temperature gradients were decreased.

Ouyang and Shyy [7] applied the continuity, momentum and energy equations to simulate the growth of β -NiAl crystal in a multi-zone Bridgman system. They have shown that the variations of the material properties need to be included in order to achieve more realistic simulations. Simulations carried out assuming constant material properties introduced significant errors.

Some recent studies were devoted to technologically important materials CdZnTe and CdTe, materials that are mainly employed in infrared detectors (see, for example, [8], [11], [12]). Kuppurao and Derby utilized the finite element method to investigate the role of support materials and ampoule geometry in influencing initial solidification and interface shape during vertical Bridgman growth of CdZnTe. They obtained that a design having a shallow cone crucible sitting on a composite support made of a highly conducting core and a less conducting outer cover gave a convex interface toward the melt.

The commercially available program FLUENT, which uses finite difference/control volume technique, was employed by Martinez-Tomas et al. to simulate CdTe growth in a vertical Bridgman furnace. Including all the system parameters and heat transfer mechanisms they obtained that there exist a significant difference between the traveling rate of the furnace and the velocity of the SL isotherm at the outset of the growth. Their results showed that the temperature field was very sensitive to the charge and ampoule peculiarities.

They also observed that the concavity of SL interface shape and the growth rate depended predominantly on the axial position of the isotherm.

In the present study, we mainly discuss the sensitivity of the energy equation on different parameters and the importance of the crucible translation rate in the utilization of the energy equation. The results obtained for different temperature profiles and radii of the crucible for different approaches to the problem are summarized and the effect of pulling rate on the slope of axial temperature profile is presented. We should note that the discussions are focused on the use and limitations of the energy equation without inclusion of other heat transfer mechanisms and detailed physical parameters of the system, such as the effect of the crucible tip and its material.

2. Theory and the Model Description

The melt and solid is contained by a cylindrical tube which is slowly lowered from a hot zone to a cooler region. The temperature within is described by a two dimensional axially symmetric energy equation for a steady, two-dimensional flow of incompressible, constant-property Newtonian fluid [15]:

$$\rho C_p \left(\nu \frac{\partial T}{\partial r} + u \frac{\partial T}{\partial z} \right) = k \left(\frac{\partial^2 T}{\partial r^2} + \frac{1}{r} \frac{\partial T}{\partial r} + \frac{\partial^2 T}{\partial z^2} \right) + k\mu\Phi. \quad (1)$$

where, T is the temperature; k is the thermal conductivity; ρ is the density; C_p is the heat capacity; u and ν are the velocity components in axial and radial directions, respectively; r is the radial coordinate; and z is the axial coordinate. One can derive Equation (1) by combining the energy balance equation for an infinitesimal volume element with the momentum equations in the absence of radiation. For unsteady flow the rate of increase of the internal energy in the volume element can be expressed by:

$$\rho C_p \frac{DT}{Dt} = \rho C_p \left[\nu \frac{\partial T}{\partial r} + u \frac{\partial T}{\partial z} + \frac{\partial T}{\partial t} \right]. \quad (2)$$

In Equation (2) the net rate of increase of the energy is obtained by considering the motion of the body in addition to the explicit rate of change with respect to time. Then the exact time dependence becomes embedded partially in the velocity components. For steady flow where the transient heat transfer is unimportant explicit time dependence can be dropped by which Equation (1) is justified. In Equation (1) the left hand side represents the net energy transfer due to mass transfer; on the right hand side, the term in parenthesis represents conductive heat transfer and the last term is the viscous energy dissipation that can be neglected when the flow velocities are moderate [15]. Neglecting also the velocity component in the radial direction and rearranging, one obtains

$$\frac{k}{\rho C_p} \left(\frac{\partial^2 T}{\partial r^2} + \frac{1}{r} \frac{\partial T}{\partial r} + \frac{\partial^2 T}{\partial z^2} \right) - u \frac{\partial T}{\partial z} = 0 \quad (3)$$

which is the equation solved by many authors (see, for example, [2], [4], [5]).

Equation (3) can also be obtained from transient heat conduction equation in a moving medium. Convective terms of components $\rho C_p T \nu_x$, $\rho C_p T \nu_y$, $\rho C_p T \nu_z$ must be added to the heat fluxes in the directions along the three coordinates, where ν_x , ν_y and ν_z are the velocity components of the moving medium. Considering that the medium moves only in z direction heat conduction equation in a moving medium can be written as [16]:

$$\frac{\rho C_p}{k} \left(\frac{\partial T}{\partial t} + u \frac{\partial T}{\partial z} \right) = \nabla^2 T. \quad (4)$$

Assuming steady state for very small velocities and writing Equation (4) in cylindrical coordinates, Equation (3) can be obtained.

In the use of Equation (3) following assumptions are made:

- i) Buoyancy in the liquid and radiation are neglected.
- ii) Latent heat liberation is neglected.
- iii) Thermal properties of the liquid and the solid are the same and independent of the temperature.
- vi) Infinitely long rod.

Defining the dimensionless parameters:

$\phi = \frac{T-T^*}{T_{\max}-T^*}$ as a dimensionless temperature, where T^* is a reference temperature; $Z = z/a$ as a dimensionless axial coordinate; and $R = r/a$ as a dimensionless radial coordinate, where a is the radius of the crucible - the dimensionless form of Equation (3) can be written as

$$\frac{\partial^2 \phi}{\partial R^2} + \frac{1}{R} \frac{\partial \phi}{\partial R} + \frac{\partial^2 \phi}{\partial Z^2} - Pe \frac{\partial \phi}{\partial Z} = 0 \quad (5)$$

where $Pe = \nu \rho C_p a / k$ is the dimensionless Peclet number. In terms of thermal diffusivity $\alpha = k / \rho C_p$, Pe number can be written as $Pe = av / \alpha$. Pe is the most important system parameter as it somehow affects the growth rate of the crystal. The method of solution of this equation and the approach to the specific problem are important concepts as they may change the effects of the system parameters on the SL interface shape and position.

On the other hand, if the explicit time dependence in Equation (2) was not neglected and used in the left hand side of Equation (1) then the dimensionless form could be written as

$$\frac{\partial^2 \phi}{\partial R^2} + \frac{1}{R} \frac{\partial \phi}{\partial R} + \frac{\partial^2 \phi}{\partial Z^2} = \frac{av}{\alpha} \frac{\partial \phi}{\partial Z} + \frac{a^2}{\alpha} \frac{\partial \phi}{\partial t} \quad (6)$$

Calling $\tau_c = a^2 / \alpha$ as the time scale of the transient response of conduction heat transfer, and $\tau_v = a / v$ as the time scale for the pulling rate, the Pe number can then be rewritten as $Pe = \tau_c / \tau_v$ resulting in the following form:

$$\frac{\partial^2 \phi}{\partial R^2} + \frac{1}{R} \frac{\partial \phi}{\partial R} + \frac{\partial^2 \phi}{\partial Z^2} = \frac{\tau_c}{\tau_v} \frac{\partial \phi}{\partial Z} + \tau_c \frac{\partial \phi}{\partial t} \quad (7)$$

The coefficients τ_c / τ_v and τ_c might be significant depending on the pulling rate, size and some properties of the grown crystal. The significance of these coefficients in the utilization of Equation (7) is discussed in the conclusion.

Considering axial symmetry, half of the crystal material can be simulated. In the radial direction m - and in the axial direction- n equally spaced points are used. Hence, indices i and j run from 1 to m and 1 to n , respectively. Central finite difference scheme is utilized to solve the dimensionless form (Equation (5)) to obtain the main expression for the dimensionless temperature at any grid point i and j , i.e:

$$\phi_{ij} = \frac{1}{4[(\Delta R)^2 + (\Delta Z)^2]} \left\{ \begin{array}{l} \phi_{i+1,j}(\Delta Z)^2 \left(2 + \frac{1}{i-1}\right) + \phi_{i-1,j}(\Delta Z)^2 \left(2 - \frac{1}{i-1}\right) + \\ \phi_{i,j+1}(\Delta R)^2 (2 - Pe\Delta Z) + \phi_{i,j-1}(\Delta R)^2 (2 + Pe\Delta Z) \end{array} \right\} \quad (8)$$

Using such a grid system and considering the imposed temperature profile at the boundary, the finite difference form of the boundary conditions can be written as:

1. at $R = 0$ (centerline) $\phi_{i-1,j} = \phi_{i+1,j}$,
2. at $R = 1$ (surface) $\phi_{m,j} = f^*_j$,
3. at $Z = L/a$ (top of the crucible) $\phi_{i,1} = f^*_1$,

4. at $Z = -L/a$ (bottom of the crucible) $\phi_{i,n} = f^*_n$,

where L is the length of the material and f_j^* is the dimensionless form of the applied temperature profile. Boundary condition 1 is substituted into the main equation to obtain the temperature at the centerline, i.e. $\phi_{1,j}$. The applied temperature profile data of our Bridgman furnace was fitted to a third order polynomial function to be used in the computations. To solve the equation for each grid point Gauss-Seidel iterative method was employed. Iteration was terminated when the difference between the current value of dimensionless temperature $\phi_{i,1}^{(s+1)}$ after the $(s+1)^{th}$ iteration and the old value $\phi_{i,1}^{(s)}$ after the s^{th} iteration passed the accuracy limit 10^{-8} [17,18].

3. Different Approaches to the Problem and Results

3.1. First Approach

We first follow a procedure similar to that of Fu and Wilcox [2] at the 2^{nd} boundary. Newton's cooling equation can be approached with

$$r = a \text{ (surface) and } -k \frac{\partial T}{\partial r} = h(T - T_e),$$

where T_e is an assumed constant temperature of the surrounding environment and h is an overall heat transfer coefficient for convection and radiation heat transfers specific to the system. The dimensionless finite difference form of this condition is

$$\frac{\phi_{m-1,j} - \phi_{m+1,j}}{2\Delta R} = Bi\phi_{m,j}, \quad (9)$$

where $Bi=ha/k$ is the Biot number and ϕ is defined using $T^* = T_e$. In this approach $\phi_{m+1,j}$ is taken as the dimensionless form of the applied temperature profile. Inserting the boundary condition (9) into the main Equation (8), we solve the problem using different values of the parameters Pe and Bi . Results showed that the Pe number is more effective than the Bi number and only for $Pe < 0.2$, from which a convex (almost flat for Pe is around 0.2) SL interface could be obtained. The Bi number seemed effective in the position of the SL interface and less effective with respect to the shape.

This approach was inadequate to describe our system for two reasons. One was that the constant reference temperature T_e that we used to define the dimensionless temperature did not represent the real environment in Newton's cooling law at the 2^{nd} boundary of the system. The second reason was that the coefficient h at the boundary depends on different heat transfer mechanisms and various system parameters, and was difficult to assign a proper value.

3.2. Second Approach

In this approach, instead of constant T_e at the boundary in the Newton's cooling law, we used the temperature profile itself at a fictitious grid point $m + 1$. The applied boundary condition then became:

$$\text{at } r = a \text{ (surface) } -k \frac{\partial T_{m,j}}{\partial r} = h(T_{m,j} - T_{m+1,j}) \quad (10)$$

where $T_{m,j}$ is the temperature on the surface of the crystal material and $T_{m+1,j}$ is the temperature profile. In this approach, we assumed that the convective boundary is at those grid points at the side of the crystal material having temperature $T_{m,j}$, and the Newtonian cooling is due to the very small difference between the temperatures of these grid points and the varying temperature profile of the furnace, $T_{m+1,j}$. Convective heat transfer coefficient h is defined more simply than in the first approach for the heat transfer between the side of the crystal and crucible inner wall surface. An assumption in this approach was that the variation of the applied temperature gradient at the crucible outer wall surface was transferred to the inner wall surface

with negligible change in its original form. Actually, we carried out experiments to test the validity of this assumption and found out that, with a few degrees decrease, the variation of the temperature profile was transferred to the inner wall surface with the same trend.

In the second approach, the new definition of the dimensionless temperature becomes

$$\phi_{i,j} = \frac{T_{i,j} - T_{m,n}}{T_{m,1} - T_{m,n}},$$

where $T_{m,1}$ and $T_{m,n}$ are the upper (maximum) and lower (minimum) temperatures obtained from the applied temperature profile.

The effect of Pe was also observed in this approach, but a slightly convex interface was obtained only for $Pe = 0$, a flat interface for $Pe \approx 0.1$ and for all the higher values of Pe interface was concave suggesting a growth rate corresponding to

$$Pe \leq 0.1. \quad (11)$$

We should note that the result $Pe \leq 0.1$ is important as it gives a maximum Pe value to achieve a flat or a slightly convex SL interface.

In this approach, effect of the Bi number could have been hardly observed, but this effect was negligible compared to the effect of the Pe number. This is due to the boundary condition (10), which is not quite different from solving the problem assuming a thermal contact between the material and the inner side of the crucible. Applying the boundary condition (10) in a central difference scheme results in an improper use of Newton's cooling law, since the temperatures at the nodes (m, j) and temperature profile at nodes $(m + 1, j)$ becomes connected through conduction.

3.3. Third Approach

The final approach is to set the temperature profile as the surface temperature of the crystal material at the second boundary instead of applying Newton's cooling law. In the definition of dimensionless temperature $\phi_{i,j}$, instead of T^* , we used the melting temperature of GaSe, with reference to Lakeenkov et al. [12]. Instead of T_{max} , we used 1200 °C, which is the highest temperature that we can use in our furnace. The results we obtained are quite similar to the results of the previous approach and following is a summary of these results.

Using different temperature profiles and different sizes of the material, temperature distributions are obtained for different Pe number. We first investigate the effect of Pe number on the dimensionless bending of the SL interface for $Pe=0.0 - 1.0$, in increments of 0.1. Dimensionless bending is defined as the difference of the dimensionless coordinate z/a between the point at the surface and at the middle of the SL interface isotherm. We found that the dimensionless bending varies linearly with Pe number as presented in Figure 1 for the temperature profile that we used for GaSe (profile B in Fig. 2). One can also observe from Fig. 1 that a convex interface can be obtained only for $Pe \leq 0.1$, as in the second approach. Note that the difference between a 0.0 bending and a slightly concave bending 0.05 ($Pe = 0.2$) corresponds to a temperature difference of 0.05 °C for results obtained with $Pe = 0.2$.

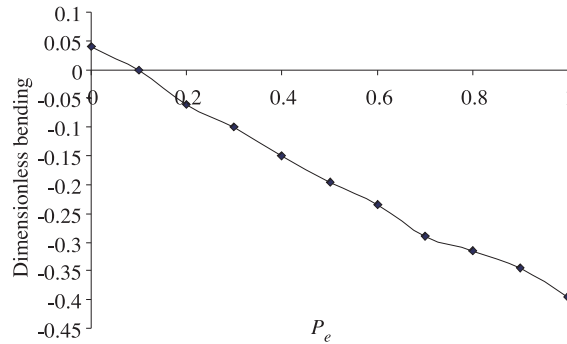


Figure 1. Variation of dimensionless bending of the interface isotherm with Pe number.

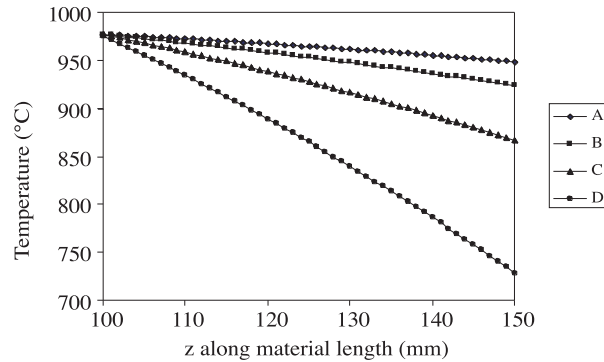


Figure 2. Applied temperature profiles.

To examine the effect of an applied temperature gradient, four different temperature profiles are generated in the form of a third order polynomial. Figure 2 shows these profiles. For all the examined profiles, dimensionless bending for different Pe numbers are almost the same, the only difference being in the position of SL interface isotherm which is shifted toward lower values of z for profiles C and D in Figure 2. We should note that the effect of different temperature profiles can be obtained in the first approach, probably due to use of Newton's cooling equation with constant ambient temperature. This effect however is also quite small, which does not considerably alter the result of promoting convex or flat SL interface for $Pe \leq 0.1$.

The shape of the crystallization isotherm depends also on the size of the crucible. The dimensionless bending decreases as the material's radius is increased with smaller rates for small Pe numbers. Figure 3 depicts this decrease for 4 different radii of the crystal for $Pe = 1$. This result is in accord with the results of Lakeenkov et al. [12]. Although the observed trends were similar to the case where $Pe=1$, the effects of radius for $Pe = 0.1$ could hardly be observed indicating that the equation in hand is not quite sensitive for a fine examination of the effects of such parameters especially for small Pe numbers.

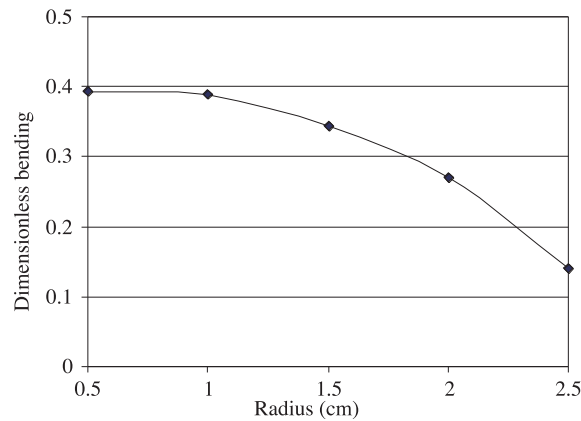


Figure 3. Effect of different crucible radius on the crystallization isotherm for $Pe = 1$ (absolute values of the dimensionless bending are used).

Figure 4 shows the axial temperature profiles (i.e. the temperature at $z=0$) for $Pe = 0$ and 1 and for length of material 5 cm obtained using the final approach with applied temperature profile B. The slope of the temperature profile increases with increasing Pe number (pulling rate) resulting in a more concave interface isotherm negatively affecting the quality of the crystal growth. However, we should point out that the change of slope is quite small even when the Pe number is varied from 0 to 1, which is a relatively large value.

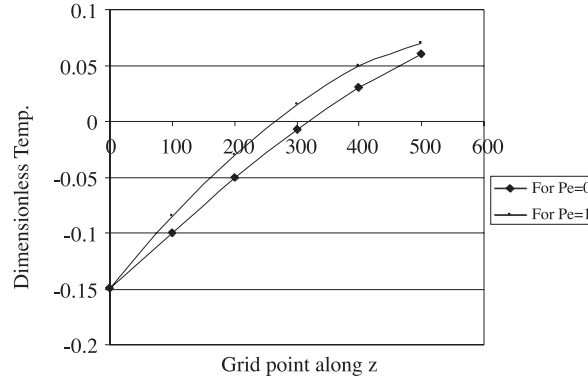


Figure 4. Axial dimensionless temperature profile for a material of length 5 cm and radius 1 cm (dimensionless temperature 0 corresponds to the melting point).

4. Conclusion

The result, Equation (11), which we obtained in the present work, might be used to determine a maximum value for the translation rate in the growth of different materials. However, due to the very small actual translation rates used in Bridgman systems for semiconductors, we concluded that only very rough upper limits of the pulling rates could be obtained using the result $Pe \leq 0.1$. Table 1 lists the values of density, thermal conductivity and specific heat of some semiconductors grown by Bridgman techniques. The values for the translation rates in the Table 1 are obtained by setting $Pe = 0.1$ for 1 cm radius crystals. As can be observed from this table, these translation rates are a few orders of magnitude larger than experimentally used translation rates. Another way of stating this fact is that the range of Pe numbers for a variety of materials is expected to be on the order of 10^{-4} to 10^{-1} [19].

Table 1. Properties of some crystals grown by Bridgman with the translation rates obtained for $Pe = 0.1$ and material radius 1cm.

Material /Prop.	ρ (gr/cm ³)	k (W/cm K)	C_p (J/gr K)	ν (mm/hr)
GaSe	5.031 [20]	0.16 [20]	0.322 [20]	355
GaAs	5.504 [21]	0.37 [24]	0.327 [21]	740
InP	4.790 [21]	0.80 [24]	0.357 [21]	1572
InAs	5.668 [22]	0.29 [24]	0.352 [21]	523
Si	2.329 [23]	0.22 [23]	0.714 [25]	476

As mentioned before, in the use of Equation (7), the magnitudes of the coefficients τ_c/τ_v and τ_c are important to decide whether the steady flow assumption is meaningful. For the typical pulling rates in the crystal growth by Bridgman systems (1-10 mm/hr) the value of τ_c/τ_v is about two orders of magnitude smaller than the value of τ_c , suggesting that the explicit time dependence in Equation (7) should not be neglected. However, for larger pulling rates corresponding to $Pe \approx 0.1$ (see Table 1) the orders of the magnitudes of τ_c/τ_v and τ_c are close so that the steady flow assumption starts to be meaningful, or in other words, the term $\partial\phi/\partial Z$ in Equation (7) becomes effective.

Equation (3) alone can give only coarse results on the effect of the system parameters on SL interface shape. Most important system parameter is the Pe number, and for a convex and/or flat SL interface, Equation (11) is the result in the second and the final approach, which may be a good indication of the limitations of Equation (3).

References

- [1] S. Sanghamitra and W.R. Wilcox, *J. Crystal Growth* **28** (1975) 36.
- [2] T. W. Fu and W. R. Wilcox, *J. Crystal Growth* **48** (1980) 416.
- [3] L. Y. Chin and F. M. Carlson, *J. Crystal Growth* **62** (1983) 561.
- [4] C. E. Huang, D. Elwell and R. S. Feigelson, *J. Crystal Growth* **64** (1983) 441.
- [5] G. L. Young, K. A. McDonald, A. Palazoglu and W. Ford, *Numer. Heat Transfer, Part A* **21** (1992) 299.
- [6] C. W. Lan and C. C. Ting, *Chem. Eng. Comm.* **145** (1996) 131.
- [7] H. Ouyang and W. Shyy, *Int. J. Heat Mass Transfer* **39** (1996) 2039.
- [8] S. Kuppurau, J. J. Derby, *J. Crystal Growth* **172** (1997) 350.
- [9] St. Boschert, P. Dold, K. W. Benz, *J. Crystal Growth* **187** (1998) 140.
- [10] C. W. Lan, D. T. Young, *Int. J. Heat Mass Transfer* **41** (1998) 4351.
- [11] C. Martinez-Tomas, V. Munoz, R. Triboulet, *J. Crystal Growth* **197** (1999) 435.
- [12] V. M. Lakeenkov, V. B. Ufimtsev, N. I. Shmatov, Yu. F. Schelkin, *J. Crystal Growth* **197** (1999) 443.
- [13] D. Morvan, M. El Ganaoui, P. Bontoux, *Int. J. Heat Mass Transfer* **42** (1999) 573.
- [14] C. E. Chang and W. R. Wilcox, *J. Crystal Growth* **21** (1974) 135.
- [15] M. N. Ozisik, *Heat Transfer-A Basic Approach* (McGraw-Hill Co., NY 1985).
- [16] H. S. Carslaw and J. C. Jaeger, *Conduction of Heat in Solids* (Oxford University Press London 1959) p. 13.
- [17] E. Akar, M. S. Thesis, Department of Physics, METU, Ankara, Turkey, 1999.
- [18] R. L. Burden, *Numerical Analysis* (PWS-Kent Pub. Boston 1989)
- [19] P. C. Sukanek, *J. Crystal Growth* **58** (1982) 208.
- [20] N. C. Fernelius, *Prog. Crystal Growth and Charac.* **28** (1994) 275.
- [21] S. Adachi, *Physical Properties of III-V Semiconductor Compounds* (John Wiley NY 1992).
- [22] Lev I. Berger, *Semiconductor Materials* (CRC Press, Boca Raton, 1997).
- [23] W. C. O'Mara, R. B. Herring, L. P. Hund, *Handbook of Semiconductor Silicon Technology* (Noyes Pub. NJ 1990).
- [24] C. M. Bhandari and A. M. Rowe, *Thermal Conduction in Semiconductors* (Wiley NY 1988).
- [25] D. R. Lide, *CRC Handbook of Chemistry and Physics* (CRC Press Boca Raton 1993).